

# The Near-Earth Object Population

Brett Gladman, Patrick Michel, and Christiane Froeschlé

*Departement Cassini, Observatoire de la Côte d'Azur, BP 4229, 06304 Nice Cedex 4, France*

E-mail: gladman@obs-nice.fr

Received February 12, 1999; revised January 19, 2000

**We examine the dynamics of a sample of 117 near-Earth objects (NEOs) over a time scale of 60 Myr. We find that while 10–20% end their lifetimes by striking a terrestrial planet (usually Venus or Earth), more than half end their lives in a Sun-grazing state, and about 15% are ejected from the Solar System. The median lifetime of our (biased) sample is about 10 Myr. We discuss the exchange of these objects between the various orbital classes and observe the creation of orbits entirely interior to that of Earth. A variety of resonant processes operating in the inner Solar System, while not dominant in determining the dynamical lifetimes, are crucial for understanding the orbital distribution. Several dynamical mechanisms exist which are capable of significantly increasing orbital eccentricities and inclinations. In particular, we exhibit important new routes to the Sun-grazing end-state, provided by the  $\nu_5$  and  $\nu_2$  secular resonances at high eccentricity between  $a = 1.3$  and 1.9 AU. We find no dynamical reason to demand that any significant component of the NEO population must come from a cometary source, although such a contribution cannot be ruled out by this work.** © 2000 Academic Press

**Key Words:** asteroids; comets; impacts; near-Earth objects.

## 1. INTRODUCTION

The near-Earth object (NEO) population consists of those astronomical bodies which are on orbits which bring them “near” the Earth. Besides being telescopically more accessible due to their occasional close passages to our planet, these objects are also of special interest because (1) their dynamical lifetimes are shorter than the age of the Solar System, and thus they must be resupplied by some more stable source (Öpik 1963, Wetherill 1979), and (2) some fraction of these objects will impact the terrestrial planets. The ultimate supply source for most NEOs is likely to be the main asteroid belt (and thus most NEOs have rocky compositions), although some undetermined fraction of the NEOs are almost certainly of cometary origin (Wetherill 1988).

Historically, these objects have been divided into the Apollo, Amor, and Aten classes, based on their current osculating orbital elements (Table I), and with the restriction of  $a < 5.2$  AU to eliminate objects with semimajor axes outside of Jupiter (like Halley or long-period comets). Below we shall refer to these three classes together as the AAA objects and the region of

orbital element space they occupy as the AAA region. Although objects change between these classes (sometimes rapidly and repeatedly) as their orbital elements vary, this classification does allow an immediate distinction between those objects which might impact Earth over a human lifespan (Atens/Apollos vs. Amors) and between those that have succeeded in making the long and hazardous journey to orbits largely interior to Earth (Atens vs Apollos).

It is clearly useful to have a class name for the as-yet undiscovered group of objects whose orbits lie entirely interior to Earth’s orbit (aphelia  $Q < 0.983$  AU), which Wetherill (1979) suggested should comprise from 1 to 3% of the NEO population. Tholen and Whiteley (1998) reported the candidate object 1998 DK36 as a potential first member of this class in a survey for Earth Trojans (Whitely and Tholen 1998), but the orbit could not be reliably established. Boattini and Carusi (1998) adopted the name Arjunas for this class; this adoption is a misuse of the term originally proposed by T. Gehrels for the small ( $< 100$  m), low- $e$  Earth-approaching objects reported by Rabinowitz *et al.* (1993). Michel *et al.* (2000) propose “inner-Earth objects,” or IEOs, which intends to indicate objects on orbits entirely interior to that of Earth’s as opposed to inside Earth. Because of this confusion, in this paper we will use the name “Anon” asteroids for this class (a whimsical abbreviation of “anonymous,” since the class will be named after its first confirmed member).

The subject of this paper is to examine the dynamical evolution of the population of NEOs as a whole, with special attention to be paid to their ultimate dynamical fate and their lifetimes. We will also attempt to say something about their origin and address issues regarding the cometary component of the population.

## 2. THE SAMPLE

In order to examine the dynamical evolution of the NEO population, we have integrated a sample of 117 cataloged objects, obtained from the catalog of Bowell *et al.* (1994), whose orbits were considered to be of high quality. Their current orbital distribution is shown in Fig. 1, where it is evident that we have only considered objects which have at the current epoch perihelia  $q < 1.3$  AU (that is, belong to the AAA classes listed in Table I). The 1.3-AU boundary created by the definition of the Amor objects is highly arbitrary; on time scales of tens of

**TABLE I**  
**Definitions of the Classes in Terms of Their Current**  
**Osculating Orbital Elements**

Class	$a$ (AU)	Other
Amor	$>1$	$1.017 < q < 1.3$
Apollo	$\geq 1$	$q < 1.017$
Aten	$<1$	$Q > 0.983$
Anon(?)	$<1$	$Q < 0.983$

millions of years the large population of Mars-crossing objects with  $q > 1.3$  AU reaches Amor, and eventually Apollo, orbits (Shoemaker *et al.* 1979, Michel *et al.* 2000). Additionally, the NEO population receives continuous feeding from the main-belt asteroid population (Migliorini *et al.* 1998), as well as some (probably smaller) contribution from the Jupiter-family comet population (Wetherill 1988). Thus, our initial sample is “unstable” in the sense that some of its members leave the region defining the population, and we expect new objects to enter the AAA regions on time scales of  $10^5$ – $10^7$  years. However, in a steady state situation this flux in and out of the population will not affect the fraction of objects which suffer certain fates; that is, we can calculate what fraction of our well-defined Apollo/Amor/Aten population terminate their lives impacting Earth (for example).

Of more concern than fluctuations across the boundaries of the AAA region is the worry that the 117 objects used are not a representative sample of the *real* objects populating this region. Telescopic observations of near-Earth objects are known to be biased against the detection of objects with high eccentricities and inclinations (e.g., Rabinowitz *et al.* 1994). Since these objects also tend to have the longest dynamical lifetimes (see discussion below) our sample may be biased toward the most rapidly evolving NEOs.

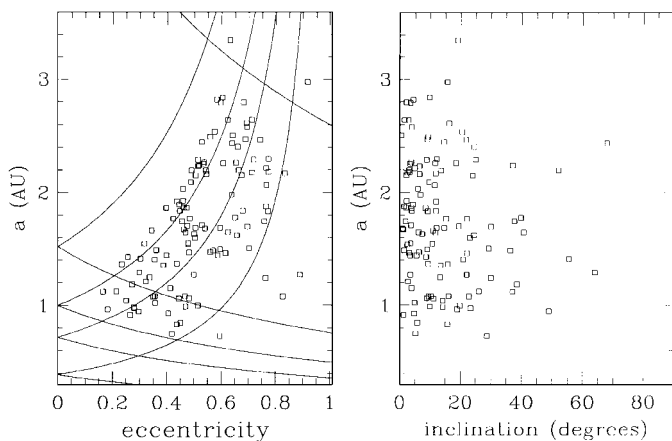


**FIG. 1.** Current heliocentric orbital elements for our 117-particle sample, used as the initial conditions for our simulation. The pericenter and node distributions (not shown) appear uniformly distributed. The curves correspond to lines of perihelia or aphelia at the semimajor axis of a planet.

Our sample was selected on the basis of orbit quality. Bottke *et al.* (1998) plot a sample of 197 Apollo and Aten objects with a less restrictive orbit-quality requirement; our Apollo/Aten distribution shows no obvious differences. Our sample did not include P/Encke, because the dynamical evolution of this comet is well studied (see Valsecchi *et al.* 1995).

### 3. APPROACH

We numerically integrated the orbital histories of our sample forward in time in order to study their dynamical evolution and the distribution of fates. A NEO typically suffers tens of thousands of planetary close approaches (within several Hill sphere radii) during a  $10^7$ -year sojourn in the inner Solar System, and so a numerical integrator for the problem must be capable of efficiently treating planetary encounters. The only numerical algorithm we are aware of that is capable of integrating a  $\sim 100$ -particle sample of planet-crossing objects for  $10^7$ – $10^8$  orbits is the RMVS3 algorithm of Levison and Duncan (1994), which is based on the symplectic integration algorithm of Wisdom and Holman (1991). We included gravitational forces only, because the orbits of kilometer-scale NEOs are presumably immune, on time scales of tens of millions of years to nongravitational (e.g., radiation pressure) or collisional effects.

The effects of all the planets except Pluto were included in the simulations. We integrated the 117 objects into two subgroups, each of about half the total sample. No differences judged to be particularly important between the evolutions of the two groups were found, implying that even a 60-object sample is large enough for the present purposes to extract some reliable information, and also implying that neither group had a significantly different initial orbital distribution. We integrated one of the groups twice, comparing the results of simulations using (base) time steps of 7.5 and 3.7 days; no differences which we believe to be significant were found between the two simulations, and so the second subgroup was integrated only with the 7.5-day time step. In reporting results below, we have used the 3.8-day step-size simulation for the first subgroup. (Note that RMVS3 automatically changes time step or reference frame in order to more accurately follow close approaches, and so the time steps reported above are actually the *maximum* used.)

Our integrations proceeded for 60 Myr of simulated time, by which time all but 19 of the original particles had been eliminated (see the next section); 11 in one subgroup, and 8 in the other. We decided that continued integration of this small sample was unwarranted.

### 4. FATES

Particles were removed from the simulation if they were ejected from the Solar System or if they impacted a planet or the Sun. The fraction of particles directly observed to finish in each of these end states is listed in Table II.

We find a very rapid decay of the number of objects with respect to time. Previous studies of long-term ( $>5$  Myr) NEO

**TABLE II**  
**Fraction of End-States for NEOs**

Fate (within 60 Myr)	Directly observed		Average prob. (%)	Impact rate, $t = 0$ rate (NEO <sup>-1</sup> Myr <sup>-1</sup> )
	$N$	%		
Impact Mercury	1	0.9	1.3	$2.3 \pm 1.0 \times 10^{-4}$
Impact Venus	12	10.1	6.8	$3.5 \pm 0.7 \times 10^{-3}$
Impact Earth	5	4.3	4.7	$4.7 \pm 1.3 \times 10^{-3}$
Impact Mars	2	1.8	0.4	$2.6 \pm 0.1 \times 10^{-3}$
Impact Jupiter	0	0.0	0.5	$2.8 \pm 2.6 \times 10^{-3}$
Impact Saturn	1	0.9	0.02	$2.4 \pm 2.4 \times 10^{-4}$
Ejected from S.S.	12	10.3	—	—
Sun-grazing	65	55.6	—	—
Survivors (60 Myr)	19	16.0	—	—

dynamics were all based on Öpik–Arnold Monte Carlo calculations of the encounter and collision time scales, based on the equations of Öpik (1976). These studies estimated the dynamical lifetime (sometimes without any analytic or numeric calculation, or reference) to be  $10^8$ – $10^9$  years (Öpik 1963), 30 Myr (Chapman *et al.* 1978), 100–200 Myr (Wetherill 1979),  $\sim 10^8$  years (Wetherill 1988), 30–100 Myr (Weissman *et al.* 1989),  $10^8$  years (Greenberg and Nolan 1989), and  $\sim 10^7$ – $10^8$  years (Rabinowitz 1997). There is room for confusion here, as some studies compute only the *partial* collision half-lives against planetary impacts (e.g.,  $\sim 10^8$  years for Shoemaker *et al.* (1979) and Bottke *et al.* (1994),  $10^7$ – $10^8$  years for Steel and Baggaley (1985),  $10^6$ – $10^8$  years for Chyba (1993)); these are correct as far as they go, but some make the implicit assumption that this is the dominant end state and thus also the median dynamical lifetime of the population, which we show below to be incorrect. As Fig. 2a shows, our direct integration finds a median dynamical lifetime of only about 10 Myr. This 10-Myr time scale has a mild dependence on the sample selection criterion; in a preliminary integration of 155 Apollo (only) asteroids with a less restrictive orbital quality criterion, we found a  $\sim 15$ -Myr median lifetime, which has been partially elevated by the presence of a larger fraction of highly inclined and  $a < 2$  particles. All the integrations show very similar (logarithmic) decay laws.

The reason for the short dynamical lifetime is easily surmised after examining Table II, which shows that over half of the particles are eliminated by the process of Sun-grazing, that is, their perihelia are lowered to the solar radius. This occurs largely because resonant phenomena, especially those operating between 2.0 and 2.5 AU such as the 3 : 1 mean-motion and  $\nu_6$  secular resonances, increase particle eccentricities to unity (Farinella *et al.* 1994, Gladman *et al.* 1997). Since most of the previous lifetime estimates relied on Öpik’s equations, which do not take resonant phenomena into account, it is not surprising that the lack of this dominant phenomenon produced long estimates for the characteristic time scale. Wetherill (1979) discussed the dangers of interpretation involved in calling this median lifetime a “half-life” since the decay is not an exponential.

To gain additional insight into the importance of the resonant phenomena, we conducted an Öpik–Arnold Monte Carlo calculation of our initial conditions using the Monte Carlo code of Melosh and Tonks (discussed in Dones *et al.* 1999). In this Monte Carlo code, no approximate modeling of some of the resonances is incorporated (as was done in varying degrees in Wetherill’s work and Rabinowitz (1997)); thus the Monte Carlo code “sees” only close encounters. Each initial condition was computed 10 times (picking different random numbers for the Monte Carlo process) and evolutions were computed for 60 Myr.

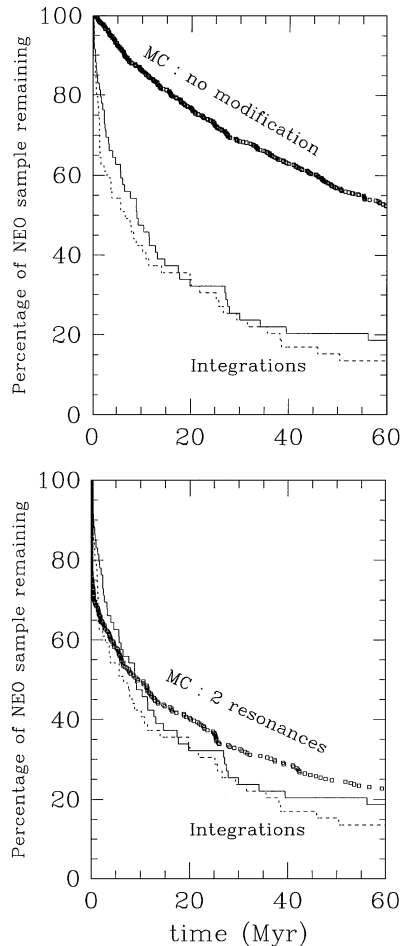


**FIG. 2.** Decay of number of integrated NEOs with time. The panels compare the results of the integrations (solid and dotted lines) with those of the Monte Carlo simulation. The two integrations correspond to the subsets of half the NEO sample. (Top) The unmodified Monte Carlo algorithm predicts a median lifetime of  $\simeq 60$  Myr, whereas the real half-life of our NEO sample is  $\sim 10$  Myr. Only close encounters are modeled in the Monte Carlo code, and so particle removal occurs only due to collisions or ejection from the Solar System (removal at  $e = 1$  is checked for, but does not occur). In contrast, most integrated particles (Table II) end their lives in a Sun-grazing state. (Bottom) We have artificially introduced a zeroth-order model of the Sun-grazing process by immediately removing from the simulation any particle which has an osculating semimajor axis of between 2.0 and 2.2 AU or between 2.4 and 2.6 AU, roughly corresponding to the  $\nu_6$  and 3 : 1 resonances, respectively.

Figure 2a shows the result of the calculation; just slightly more than half of the particles remain after 60 Myr, a much lower mortality rate than observed in the integration.

A question we find interesting is: what is dominantly determining the 10-Myr time scale of the population? We know that resonant phenomena are important in the 2.0- to 2.5-AU region, and it is clear from the end states and from the evolutions (see next section) that the particles mostly terminate their evolution by solar collisions in this region. However, how are NEOs moved from the evolved region ( $a < 1.8$  AU, see Gladman *et al.* 1997) out past 2 astronomical units? Are resonant phenomena important to this process? We answered these questions by running a second Monte Carlo calculation, in which we (rather harshly) approximated the resonance regions by “traps” between 2.0–2.2 AU (for the  $\nu_6$ ) and 2.4–2.6 AU (for the 3:1); any object entering one of these traps was immediately eliminated from the simulation. This approximation has the known shortcomings that (1) the semimajor axis of the center of the  $\nu_6$  is inclination dependent, and (2) particles can escape resonances before being eliminated. However, if even this dramatic “death’s door” approach failed to bring the decay rate of the Monte Carlo simulation down to at least as fast as the integration, we would have proof that resonant phenomena inside  $a = 1.8$  AU are crucial for delivering NEOs out to the Sun-grazing region. In fact, Fig. 2b shows that this rough model brings the two simulations into decent agreement. The abrupt drop at the start of the modified Monte Carlo simulation results from the immediate elimination of all particles in the “resonant regions,” after which the decay law is only slightly slower than in the integration. The number of impacts detected in the “modified” Monte Carlo simulation drops by about a factor of 3, with these particles dominantly redirected into Sun-grazing fates.

Therefore, to a first approximation, the general picture of NEO evolution consists of these objects being dominantly controlled by close encounters while interior to 1.8 AU, which then deliver them to the region of powerful resonances exterior to 2 AU, where they are efficiently disposed of, mostly into the Sun. This result was not clear before this work, since it was known that secular and mean-motion resonances operate (and are frequently seen in numerical integrations) inside 2 AU (Michel and Froeschlé 1997, Gladman 1997). However, sometimes these resonances serve as sources of meta-stability by temporarily extracting particles onto regions where close encounters are less frequent, while in other cases they are able to take particles from meta-stable regions into quickly evolving ones (Michel and Froeschlé 1997, Gladman *et al.* 1997). The result of this comparison with the Monte Carlo model allows us to conclude that on average these effects tend to cancel out for the purposes of semimajor axis transport, and that the lifetime of the population is set by the rate at which close encounters deliver the population out to  $a > 2$  AU. The reader should *not*, however, conclude that resonant effects are not important for determining the orbital distribution of the NEOs, as we shall show below.

#### 4.1. Impacts

Due to the efficient destruction of the NEO population by delivery to Sun-grazing orbits, only a minority ( $\sim 10$ – $15\%$ ) actually impact a terrestrial planet (Table II). In our integrated sample of 117 NEOs we found 21 planetary impacts in our 60-Myr experiment, and it is likely that a similar 10–20% of the 19 surviving particles would end their evolutions in impacts. Since there are only 21 directly observed impacts, deriving statistics for the relative impact rates on the planets is difficult due to small number statistics; for example, is the larger number of venusian impacts (12) relative to Earth impacts (5) significant if they both have  $\sqrt{N}$  errors? The answer, even at only the  $2\sigma$  level, is no.

In order to place this discussion on a firmer footing, we have employed a procedure first used in Morbidelli and Gladman (1998) to calculate an “expected number of impacts” from a sample of orbital histories. Our numerical integrations have the osculating orbital elements of all surviving test particles recorded every 5 or 10 thousand years, and thus we have a set of “snapshots” of the time evolution of the orbital distribution. For each of these output intervals, we compute the collisional probability of the surviving population with each planet using a numerical code of Farinella and Davis (1994) based on the algorithm of Wetherill (1967). This algorithm computes “average” collision probabilities in the sense that the orbits of both the target planet and the particle are assumed to uniformly precess through a complete precessional cycle of the node and pericenter; some of the NEOs may have their orbits change on time scales shorter than this (few  $\times 10^4$  years), so this procedure is only approximate.

The algorithm applied gives results which are consistent with the number of directly observed impacts when the latter are also large enough to be statistically reliable (Morbidelli and Gladman 1998), and when the majority of particles are not in orbits almost identical to that of a planet (Dones 1999). Figure 3 reports the *cumulative* impact probability of the integrated sample of particles with Earth for three simulations; this quantity is identical to the average number of impacts we expect to have recorded in the simulations as a function of time, for all three numerical simulations performed. In contrast to the similar decay in the number of particles with time (Fig. 2), which is in all three cases determined on a roughly 60-particle sample, the number of expected impacts is determined by the relatively small number of particles ( $\sim 5$ – $15$ ) in each simulation that live for significant amounts of time in the Earth-crossing state. A comparison with the observed number of impacts in this case (see figure caption) shows acceptable agreement. Upon inspection, it was seen that the two simulations which shared the same initial conditions exhibited slightly different orbital distributions over the duration of the simulation; the integration with the shorter time step had many of its long-lived particles remaining for an extended period in Earth-like orbits, while in the other integration many of the longest-living particles were removed from the Earth-crossing state between  $t = 10$  Myr and  $t = 20$  Myr, explaining the differences in the impact statistics. The quantitative results

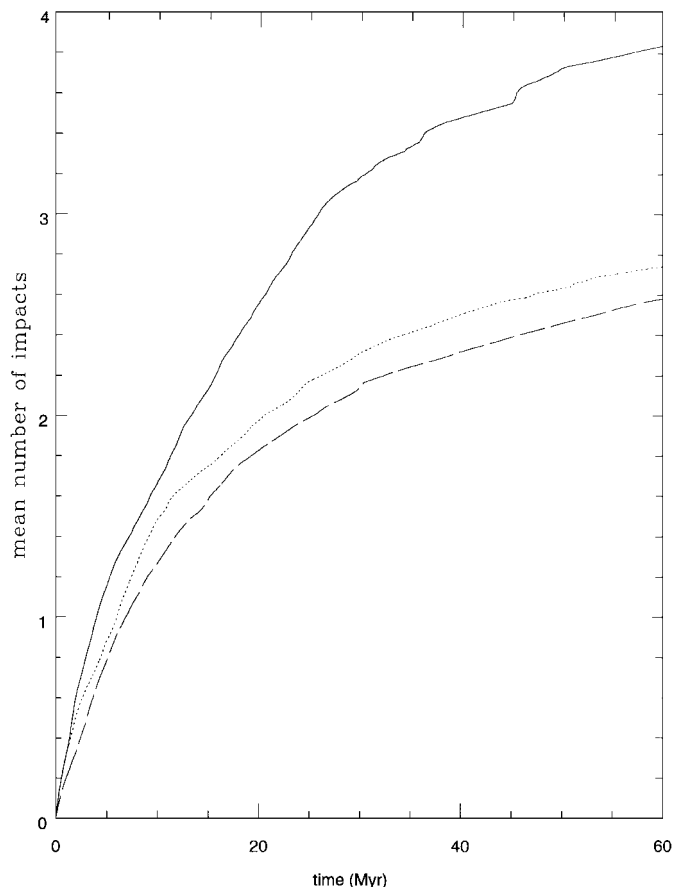


**FIG. 3.** The cumulative collisional probability with Earth, and thus the average number of impacts expected, for our three numerical simulations. The dashed and dotted curves show results for the two 7.5-day step-size simulations, while the solid curve gives the result for the 3.8-day time step (the same initial conditions as the dotted curve). From top to bottom, the number of impacts directly recorded in the simulations was 4, 2, and 1. See text for discussion.

on the impact probability are thus poorly determined compared to the median lifetime, since we are forced to base them on a small number of particles. The three integrations show generically similar behavior, and we estimate the collision results to be accurate to a factor of 2.

Table II compares the percentage of directly observed impacts (over 60 Myr) with the fraction expected from the probability algorithm; given Poisson errors for the number  $N$  of observed impacts, the results are statistically identical to the direct integration. This similarity of the number of detected collisions with that predicted by the Öpik equations in the collision probability algorithm indicates that in those cases where Öpik–Arnold Monte Carlo algorithms fail (see Dones *et al.* 1999), it is *not* due to the fact that the Öpik formulae incorrectly calculate the close-encounter probability, but rather that the orbital evolutions predicted via the patched conic approach are in error. As discussed in Dones *et al.* (1999), because of finite sampling of the orbital histories the collision probability algorithm may under-

estimate the actual collision rate by a relative error of 10–30%, due to the sampling missing the rare states of very high collision probability.

The cumulative collision probability plots provide, via their slope, the evolution of the impact rate with the planet versus time. The current impact rate of *our sample* of NEOs can be estimated by the initial slope, which is roughly constant for the first few million years. Because of the finite number of particles, we have estimated these impact rates by extracting the mean number of impacts expected after 1 Myr and dividing by the number of particles to obtain the expected impact rate per Myr per NEO (Table II). We have estimated the error on this result by computing the mean of the impact rate provided by the two samples, and quoting an error of the difference between that mean and either sample.

The impact rate per year onto a given planet can now be obtained by multiplying the estimate given in Table II by the reader’s preferred value for the number of objects in the NEO population larger than a certain size. Using an estimated population of  $\sim 2000$  Earth crossers larger than 1 km (Rabinowitz *et al.* 1994), one predicts impact rates similar (to within a factor of 2) but slightly higher than previous published values (e.g., Steel and Baggaley 1985, Wetherill 1989, Morrison *et al.* 1994). Using the most recent unpublished estimates of  $750 \pm 250$  (Rabinowitz *et al.* 2000, Bottke and Morbidelli pers. commun.), produces values more comparable to the previous estimates. The interpretation is complicated due to the fact that when integrated over a million-year time interval our population “smears” in orbital element space as objects move in and out of especially high collision probability states. Since it has been remarked by many authors (e.g., Milani *et al.* 1990, Chyba 1993) that the current collision probability is dominated by the few highest probability objects, which will not stay in this state for very long, we suggest that our impact rates may be a better representation over the time scale of precessional motions in the near-Earth space. Of course, because our rates are computed using our biased sample, these  $t = 0$  rates must be cautiously interpreted; for example, the venusian impact rate calculated this way must be an underestimate since there are doubtless undiscovered Venus-crossing asteroids with orbits in the Anon class. Additionally, the inefficiently discovered Aten asteroids have higher intrinsic collisional probability with Earth (Steel and Baggely 1985), and thus are underrepresented in our computation. Last, our calculations address only the impact rate *from the NEO population* and ignore the contribution from the Earth-crossing long- and short-period comets.

We can also compute the distribution of average impact velocities using the same algorithm which calculated the collision probability. Bottke and Greenberg (1993) discuss a superior method which computes instantaneous collision probabilities for a sample. We compute the average encounter velocity (which varies slightly due to the eccentricity of Earth’s orbit) weighted by the average collision probability in order to compute the distribution of impact velocities. Figure 4a shows the distribution

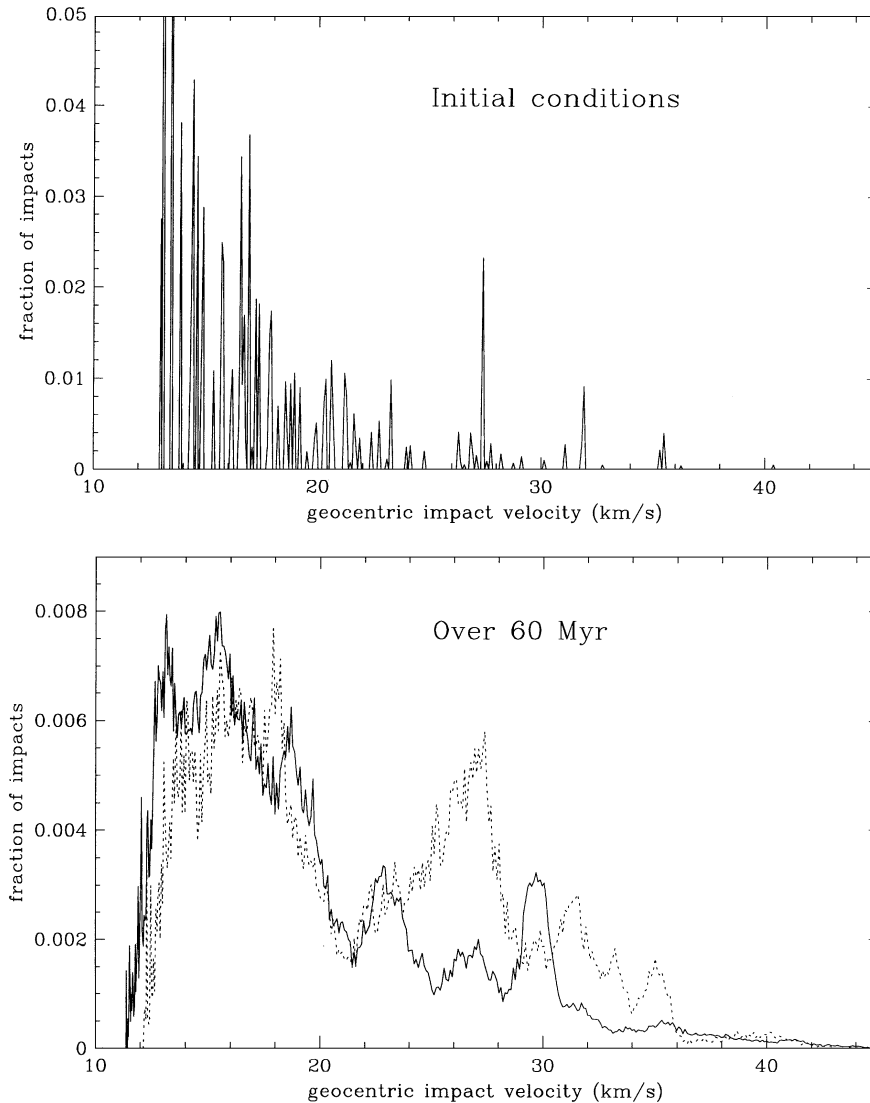


**FIG. 4.** Distribution of Earth-impact velocities, both for initial conditions of the 117-particle sample (top) as well as for the two subsamples integrated over the 60-Myr integration. The ordinate represents the fraction of Earth impacts that would occur at the corresponding velocity (normalized to unity for each distribution). The difference between the two integrated distributions reflects the finite sampling of a relatively small number of particles. The median impact velocity is 15 km/s for the initial conditions, and 19 km/s for the average of the two integrations.

of averaged Earth-impact velocities for an initial sample of 59 particles, which compares favorably with that shown by Bottke *et al.* (1994, Fig. 8). Figure 4b shows the same result when computed over the entire lifetime of the sample; this result is interesting because it is not clear a priori how it would differ from the initial distribution. Would the Earth-like orbits with low encounter velocities quickly be removed, biasing the distribution to higher velocities? Or would the NEOs which contribute most to collision probability, i.e., those with the most Earth-like orbits and hence lower encounter velocities, dominate as they transit through this rare state? Figure 4b shows that apparently the former effect is slightly more important. The reader is cautioned to not interpret the integrated distribution as the true steady-state distribution of impact velocities, since the objects

we have integrated in the AAA region are quickly resupplied from the various source reservoirs (see Gladman *et al.* 1997, Migliorini *et al.* 1998). In fact, assuming that it is representative of the entire (as yet incompletely discovered) NEO population, it is the impact distribution of the *initial* sample that best reflects the steady-state distribution (assuming the latter concept does indeed apply to the current population). The comparison of the two impact velocity distributions indicates that if the detection bias varies significantly as a function of orbital elements (as seems to be the case according to Rabinowitz *et al.* (1994) and Jedicke and Metcalfe (1998)) then the inefficiently discovered non-Earth-like orbits (with high impact velocities) are a more important component of the impact velocity distribution than implied by computing this distribution from the currently known

objects. We have calculated the steady-state impact velocity distribution for a large sample of test particles initially placed in the 3 : 1 resonance (see Morbidelli and Gladman 1998); this distribution contains a larger fraction of impact velocities above 20 km/s, implying that if this resonance is the ultimate source of NEOs then the detected sample is heavily biased against finding objects in the resonance at  $a = 2.5$  AU.

Although the statistics internal to these NEO simulations are not strong enough to establish the result, we have noted that in a wide variety of other simulations done by our group the cratering rate per unit time on Venus is slightly ( $\sim 30$ – $50\%$ ) larger than that on Earth. In the present simulation we note that even though our sample is biased against Atens and does not include the undoubtedly existing population of solely Venus-crossing asteroids, we still find (Table II) more Venus impacts. We suggest that this difference is predominantly due just to the shorter orbital period of Venus, since collision probabilities per unit time scale as the planetary  $a_{\text{pl}}^{-3/2}$  (Öpik 1976), rather than anything fundamentally related to the orbital distribution. This somewhat larger venusian cratering rate has important implications for the age of the planetary surface (see McKinnon *et al.* 1997 for a discussion), pushing the ages of cratered surfaces down.

## 5. EVOLUTION TYPES

We now proceed to examine the types of orbital evolution, and some specific cases, exhibited in our sample. We visually examined the orbital histories of the osculating elements and all the secular arguments  $\nu_2$ – $\nu_6$  and  $\nu_{12}$ – $\nu_{16}$  for all of the integrated particles. One is naturally led to ask the question if a more useful classification of the orbital behavior than Apollo/Amor/Aten could be developed, in the spirit of the Milani *et al.* (1989) Spaceguard classification, which was roughly valid over  $10^5$ -year time scales. However, we have found no useful classification for our particles on the 10-Myr time scales which the particles voyage throughout the NEO region. The Tisserand parameter does not provide a useful discriminant over these time scales (Gladman *et al.* 1997) due to the chaotic nature of the orbits and the plentiful presence of resonances in the inner Solar System (Michel and Froeschlé 1997). In the end we have decided to remain with the AAA classification, which at least has the virtue of delimiting Earth-impacting behavior over short time scales.

Figure 5 shows how the number of members of each of these classifications evolved with time for a 59-particle sample, either due to changing class or leaving the integration. There is nothing of great interest here, except to note that it is the abundant Apollo population that most closely follows the decay law of the full population, largely because only Apollo objects become Sun-grazers. Some objects clearly escape into the non-AAA region of non-Earth-crossing orbits outside the  $q = 1.3$  AU line, where they tend to be somewhat more stable. We note the transfer of a few objects into the Anon class; the rapid transfer of some objects into this class implies it is of order 1–5% of the total

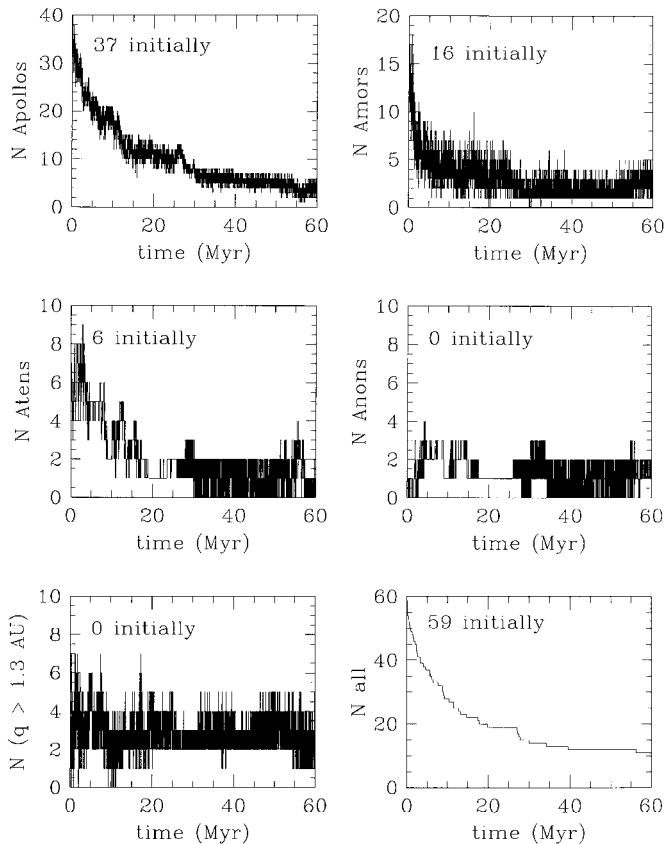


**FIG. 5.** Number of particles in the various orbital classifications (see Table I for definitions) as a function of time.

AAA population, in agreement with Wetherill’s (1979) estimate. Michel *et al.* (2000) estimate that 6–7% of the AAA population would be in the Anon class in a steady state if they were supplied from a Mars-crossing source.

The variety of orbital evolutions exhibited in our sample is very large. Below we will attempt to summarize some of the most important types of behaviors, which seem to be the most important to the evolution of the overall population. There are many interesting specific cases, illustrating dynamical processes operating in the inner Solar System, that we will not discuss here due to space limitations.

An example of the common Sun-grazing fate is given in Fig. 6, which serves as a typical example of how NEOs arrive and leave the terrestrial region. Beginning at  $a = 2.3$  AU, this object suffers several close encounters which random-walk its semimajor axis down to just outside the orbit of Mars. This object is then extracted into the Amor region (see section below) and eventually reaches a nearly circular orbit exterior to Mars; the secular effects of the  $\nu_3$  and  $\nu_4$  resonances are important during this process. After a residence at low eccentricity it is again the  $\nu_3$  and  $\nu_4$  resonances which deliver the object to an Earth-crossing orbit, after which close encounters deliver it to the resonances outside 2 AU, which drive it into the Sun (in this case the ultimate culprit

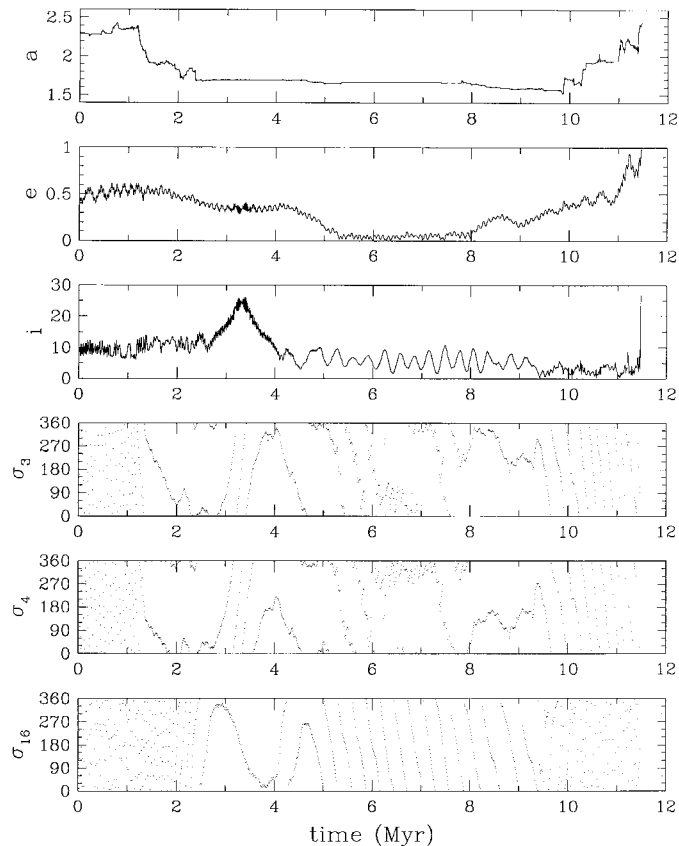


**FIG. 6.** Evolution of an object which terminates with a solar collision. From top to bottom we show the time evolution of the semimajor axis (AU), eccentricity, inclination (degrees), and the critical arguments for the secular resonances  $\nu_3$ ,  $\nu_4$ , and  $\nu_{16}$ . These secular arguments are defined by  $\sigma_3 = \varpi - (g_3t + \alpha_3)$ ,  $\sigma_4 = \varpi - (g_4t + \alpha_4)$ , and  $\sigma_{16} = \Omega - (s_{16}t + \beta_6)$ , where  $t$  is time,  $\varpi$  and  $\Omega$  are the particle's longitude of perihelion and ascending node,  $g_j$  and  $s_j$  are the proper secular frequencies of the Solar System (see Laskar 1990), and  $\alpha_j$  and  $\beta_j$  are the latter's initial phases.

is the 3 : 1 resonance). We shall discuss inclination oscillations caused by the  $\nu_{16}$  resonance in Section 5.2.

### 5.1. New Routes to Sun-Grazing

It has already been well-established that the dominant end state for planet-crossing objects with  $a > 2$  AU is solar impact (Farinella *et al.* 1994, Gladman *et al.* 1997). We have established above that even NEOs beginning with  $a < 2$  AU also predominantly terminate their evolution by migrating out to  $a > 2$  AU and being raised to  $e = 1$  by well-established resonant phenomena.

However, we have identified in the present integrations another route to Sun-grazing which occurs while objects have  $a < 2$  AU. Ten percent of our initial conditions suffer this fate. The  $\nu_2$  or  $\nu_5$ , and sometimes the overlapping of both, produce eccentricity oscillations capable of producing perihelia smaller than the solar radius for a range of semimajor axes between

$a = 1.3$  and 1.9 AU. Figure 7 gives an example of this evolution, where it is the  $\nu_5$  resonance that is clearly responsible for the large-scale eccentricity oscillations at high  $e$ . These resonances have not been located at such high eccentricities before, since semianalytical methods (Morbidelli and Henrard 1991, Michel and Froeschlé 1997) break down due to the occurrence of nodal crossing during orbital precessional cycles, nor have they been identified numerically to our knowledge. Of minor note is that if the additional 10% of the initial conditions terminating in this fate were removed from Fig. 2b, the Monte Carlo simulation would come into even closer agreement with the direct integration. We thus conclude that a combination of planetary close encounters and the  $\nu_2$  or  $\nu_5$  resonances supply a route to Sun-grazing independent of the known processes operating outside 2 AU.

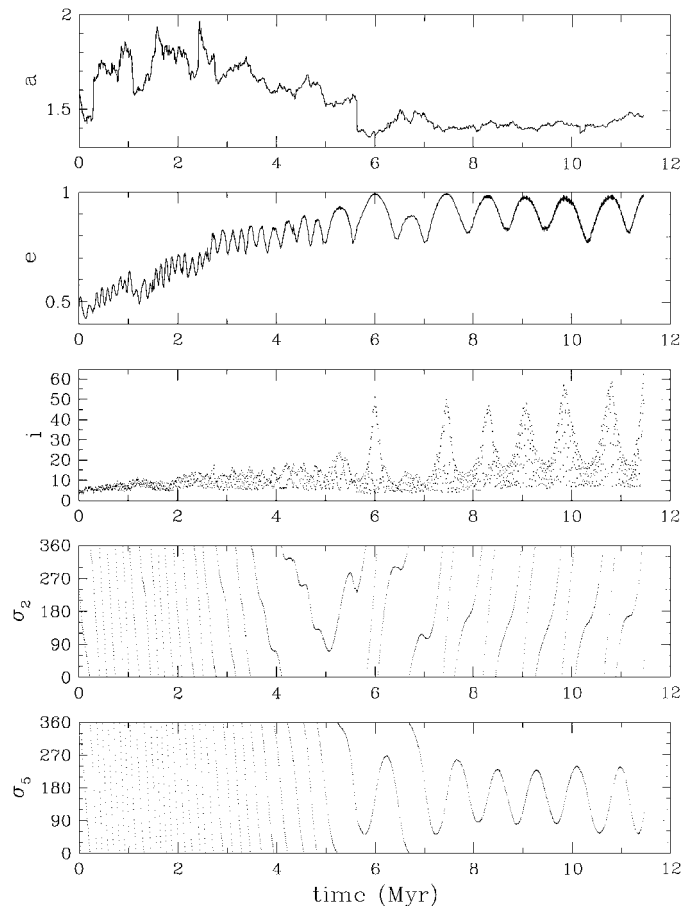


**FIG. 7.** An example of a particle driven to a Sun-grazing orbit inside  $a = 2$  AU. Close encounters with Earth and Venus appear to be the cause of the initial increase in eccentricity before  $t = 4$  Myr. The particle then passes through the  $\nu_2$  resonance, which pushes the mean eccentricity even higher so that the  $\nu_5$  resonance is entered. The eccentricity oscillation is then perfectly in phase with the libration of the  $\sigma_5$  secular argument, and mild close encounters modulate its amplitude until solar collision occurs. At the high  $e$  portions of the  $e$  cycle it is the Kozai resonance which temporarily produces the large inclination variations.

## 5.2. Inclinations

It has long been known that the AAA population contains a larger fraction of high-inclination orbits than the main asteroid belt (Wetherill 1988, Weissman *et al.* 1989). We discuss below in Section 6 the important argument that this implies a cometary source for these highly inclined NEOs. Here we show that resonant phenomena in the inner Solar System appear capable of taking low-inclination orbits from an asteroidal source (in fact, from any source) and increasing their orbital inclinations well above  $30^\circ$ .

Figure 8 shows an example of this process. This NEO begins on a low inclination orbit which then undergoes moderate amplitude oscillations in the Amor state caused by the  $\nu_{13}$  and  $\nu_{14}$  secular resonances near  $a = 1.4$  AU; the inclination where this occurs ( $10^\circ$ ) is that predicted semianalytically by Michel and Froeschlé (1997). Close encounters then produce an Earth-crossing particle which random walks the semimajor axis be-

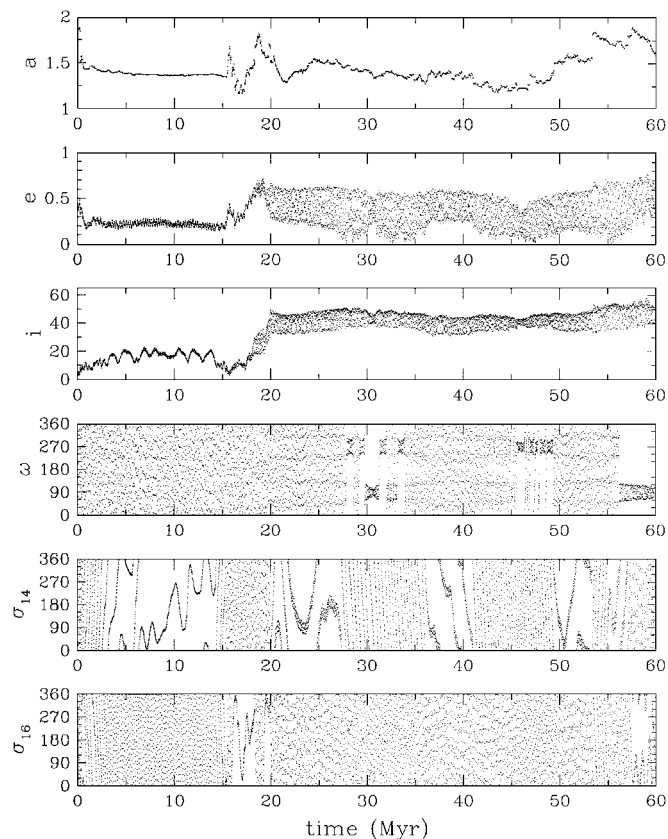


**FIG. 8.** Time evolution of a NEO which has its orbital inclination dramatically increased by resonant phenomena, in this case the  $\nu_{14}$  and  $\nu_{16}$  secular resonances. The  $\sigma_{13}$  resonant history (not shown) is similar to that of  $\sigma_{14}$ , indicating an overlapping of the two (Michel 1997). The argument of pericenter  $\omega$  serves as the critical argument for the Kozai resonance which causes the  $e$  and  $i$  oscillations after 20 Myr; particles in this high  $e/i$  state tend to be long-lived. The eccentricity increase between 17 and 18 Myr is caused by the  $\nu_2$  resonance (not shown). See text for further discussion.

tween 1.2 and 1.8 AU. During this process the particle's inclination is strongly affected by the  $\nu_{16}$  resonance, which quickly raises the mean inclination from  $10^\circ$  to  $40^\circ$ . Wetherill (1988) suggested that this resonance may be capable of producing the NEOs with inclinations  $>30^\circ$ , and we confirm that not only is this process possible, it is in fact very common. We show in Section 6 the inclination distribution produced by the totality of inclination-pumping mechanisms as particles journey into the NEO region.

Besides  $\nu_{16}$ , the overlapping of resonances  $\nu_{13}$  and  $\nu_{14}$  is capable of producing  $\sim 10^\circ$ -amplitude oscillations in the inclinations, as illustrated in Fig. 8 from  $t \simeq 5$ –15 Myr and as discussed in Michel (1997). We rarely observe these two resonances producing inclinations larger than about  $30^\circ$ . However, their presence is important because they serve as a “bridge” between  $i < 10^\circ$  orbits (which they can pump to  $i \simeq 20^\circ$ ) and the  $\nu_{16}$ 's action at even higher inclinations.

One of the few general behaviors seen in the integrations is the (unsurprising) relatively long lifetime of NEOs which begin in or eventually reach orbits of high eccentricities ( $e > 0.6$ ) or inclinations ( $i > 40^\circ$ ). These orbits tend to be longer lived since planetary close encounters then occur at high relative velocity, meaning that only small orbital changes are possible during the close encounter. If the NEO enters such a state without strong resonant phenomena nearby, then it can remain there for time scales of tens of millions of years. Figure 8 gives an example of such an object, which also illustrates that such objects can suffer out-of-phase oscillations in  $e$  and  $i$  due to the Kozai resonance (Michel and Thomas 1996); however, the relative stability of these states is provided by the high inclination and not by the Kozai resonance. Because such high inclination/eccentricity orbits are less likely to be discovered due to observational biases, and because they are seen to be populated in our simulations for long periods, we predict that there is a substantial population of such objects in the NEO region.

## 5.3. Amor Creation

The origin of Amor asteroids and of Mars-crossing asteroids exterior to the Amor region (i.e.,  $q > 1.3$  AU) has been recently discussed by Migliorini *et al.* (1998) and Michel *et al.* (2000), who calculate that the current population of large Mars-crossing asteroids ( $D > 5$  km) may be able to replenish the Earth-crossing population in this size range over its dynamical lifetime, thus keeping the Earth-crossing population in steady state. Here we address only the specific question of how most Amor asteroids with semimajor axes smaller than the inner edge of the main-belt ( $a < 2$  AU) arrive in that region of orbital element space. There would seem to be two main possibilities:

(1) Asteroids have their eccentricities increased to Mars-crossing orbits by resonant phenomena, and are then removed from the resonances and transported to smaller  $a$  by martian close encounters (Greenberg and Nolan 1989, see Fig. A2 of Bottke *et al.* 1996). Note that Öpik (1963) showed that this

process alone cannot then supply the Apollo asteroids (which in this model reach Earth-crossing orbits only via martian close encounters); the time scale for this process is so long that the ratio of Amors to Apollos would be much larger than observed. Unlike Öpik, we now know that resonance can *also* increase  $e$ 's to Earth-crossing values, so perhaps Amors could just be the small fraction of the asteroids "removed" by Mars and transported by close encounters to  $a < 2$  AU. However, Gladman *et al.* (1997) showed that this is an extremely rare and inefficient process.

(2) Rather, the dynamics produce  $a < 2$  AU Amors via the "extraction" by resonant phenomena of Apollo asteroids from Earth-crossing orbits (cf. Michel *et al.* 2000). Figure 9 shows an example. The  $\nu_3$  and  $\nu_4$  resonances are often important in this process, as in the case shown in Fig. 9 (cf. Fig. 6). Gladman (1997) discusses two second-order secular resonances in this region, originally located by Morbidelli and Henrard (1991), which can produce similar effects. Once extracted, these objects often remain decoupled from Earth for millions to tens of mil-

lions of years. These Amors are returned to Earth-crossing orbits by the same resonant processes which extracted them.

#### 5.4. The Near-Earth Region

Although we observe cases of the production of Earth-like orbits via resonant phenomena and close encounters bringing objects down to  $a \simeq 1$  AU,  $e < 0.2$ , and small  $i$ , we see no evidence of any kind of dynamical mechanism which would tend to concentrate objects in this region (cf. Bottke *et al.* 1996). Figure 10 shows an example of such an object, whose orbital history we plot in  $a/e$  space. Does the proposed population enhancement in the "SEA" (or "Arjuna") region  $0.9 < q < 1.1$  AU and  $Q < 1.4$  AU (see Rabinowitz *et al.* 1993, Rabinowitz 1997) imply an unknown source, a recent near-Earth event, or nonequilibrium feeding from the main belt (Rabinowitz 1997), or is it an artifact of detection biases (Jedicke and Metcalfe 1998)?

## 6. ORIGIN

What fraction of the NEOs are actually devolatilized comet nuclei? This is a difficult topic for the following reasons. We know that there is at least one active comet (Encke) in an NEO orbit, proving the existence of such a population (Weissman *et al.* 1989). Input flux calculations seem to imply that at least half of the NEOs can be supplied by the main asteroid belt (Wetherill 1988 and references therein, Migliorini *et al.* 1998, Menichella *et al.* 1996) and could perhaps provide effectively all of the estimated 750–2000 objects with  $D > 1$  km (Rabinowitz *et al.* 1994, Rabinowitz *et al.* 2000). However, calculations of the input flux (in number of NEOs per unit time) from the main belt are fraught with complications which yield it difficult to be more accurate than a factor of two, always leaving space for an almost equal cometary component. Also, the injection rate of one comet-like Encke every 60,000 years (e.g., Wetherill 1988) may seem relatively modest.

However, to our knowledge no one has demonstrated the decoupling of an object starting on a Jupiter-Family comet (JFC) orbit into the non-Jupiter-crossing region for any significant length of time ( $> 10^5$  years) under purely gravitational dynamics. Harris and Bailey (1996) found two examples of transient (1000–3000 years) decoupling to perihelia with  $4.0 \text{ AU} < Q < 4.2 \text{ AU}$ , but which returned to Jupiter-crossing thereafter; they estimate an upper bound to the transition probability from JFCs to decoupled NEOs of  $3 \times 10^{-3}$ . Levison and Duncan (1994) also found some examples of temporary decoupling into the NEO region (for  $10^3$ – $10^5$  years). Clearly close encounters with the terrestrial planets provide a method for doing this, but the probability of this very rare event is difficult to estimate. Valsecchi *et al.* (1995) show a purely gravitational orbit which transits from the JFC region to the decoupled region, obtained by integrating the NEO 2212 Hephaistos until it reached a JFC orbit and then inverting time (since Newton's equations are time reversible), but this method of course cannot provide the probability of a transition from JFCs to Encke-like orbits.

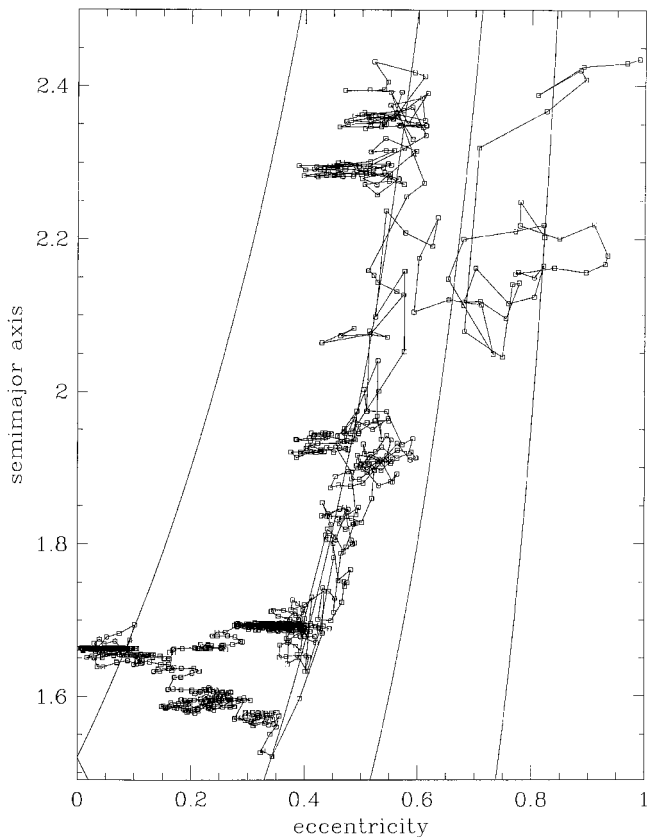


**FIG. 9.** An example of the temporary creation of long-lived Amor and Mars-crossing orbits, for the object shown in Fig. 6. The NEO begins at  $a = 2.3$  AU and journeys down to be extracted from Earth-crossing space, reaching an almost circular orbit just exterior to Mars. The curves show loci of perihelia at each terrestrial planet; this object spends a fair amount of time with  $q = 1$  AU. Squares are orbital elements sampled at  $10^4$ -year intervals.

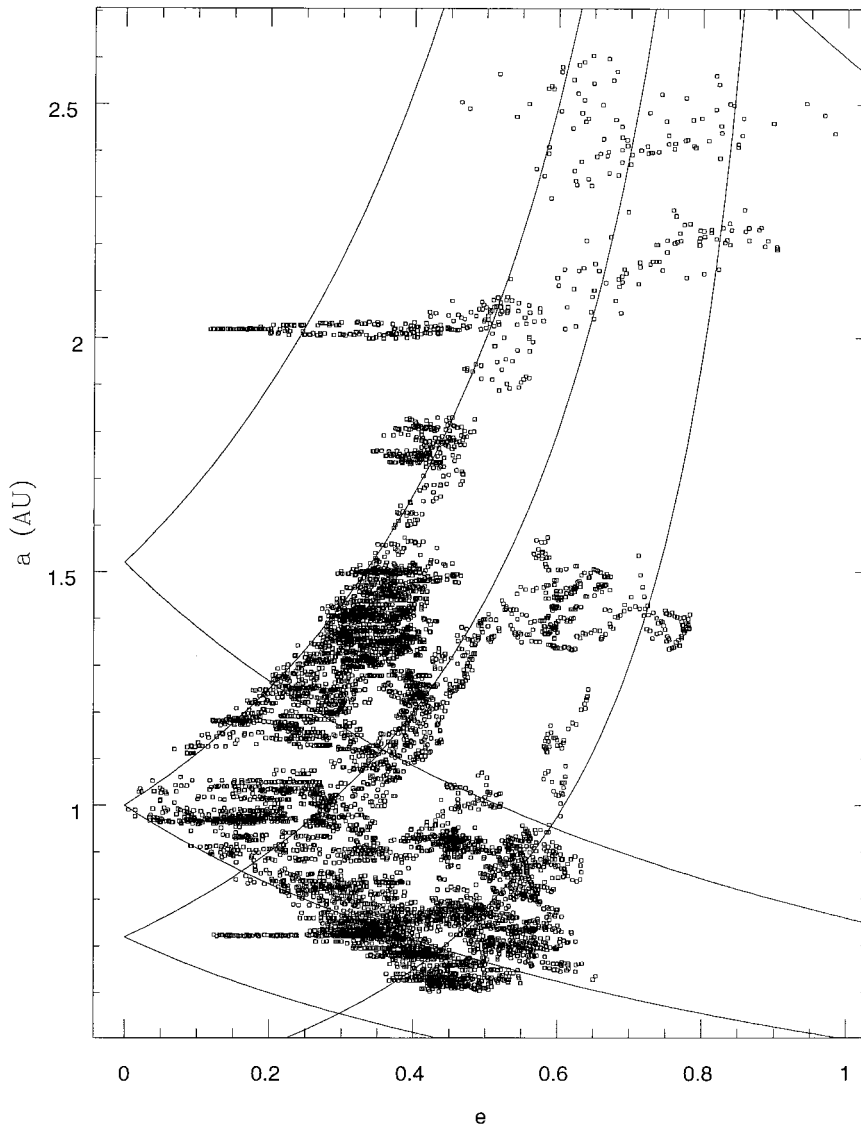


**FIG. 10.** An example of a NEO which resides temporarily in the “SEA” region. Though this particle spends some fraction of its time with  $0.9 < q < 1.1$  AU and  $Q < 1.4$  AU, it does so in several short visits, continuously entering and exiting this region. In fact, a much longer time is spent in the Aten/Anon region, for a short visit to the  $\nu_6$  resonance (horizontal feature at  $a \simeq 2$  AU) and then is finally pushed into the Sun by the 3:1 resonance ( $a = 2.5$  AU). Notice that the excursions into the  $Q < 0.983$  AU Anon region are dominantly caused by resonant phenomena decoupling the aphelion from Earth.

It is sometimes postulated that nongravitational forces may be able to lower the perihelia and thus decouple comets which are just marginally Jupiter crossing (Valsecchi *et al.* 1995, Harris and Bailey 1996, Steel and Asher 1996). Valsecchi (1999) reviews this problem. These forces are difficult to study systematically because they appear to be highly variable from comet to comet (Marsden *et al.* 1973). Harris and Bailey (1998) use the Marsden *et al.* (1973) model to simulate the orbital evolution of a sample of test particles all with initial orbital elements of  $q = 1$  AU,  $Q = 5.2$  AU,  $i = 0^\circ$ , finding  $\sim 3\%$  of the objects “decoupling” from Jupiter within  $10^3$  perihelion passages and concluding that 300 decoupled NEOs could be produced per million years. However, the assumed initial distribution is un-

realistic and is essentially “perfect” to maximize the effects of the nongravitational forces; the real fraction of Jupiter-family comets that undergo this decoupling must be at least an order of magnitude lower.

Our integrations show that dynamical mechanisms exist in the terrestrial planet region which are capable of pumping inclinations of low- $i$  objects to values like those exhibited by the NEO population. Thus, there is no a priori reason to favor comets over asteroids as the source objects because it may seem easier to supply the high- $i$  NEOs from JFC orbits (Weissman *et al.* 1989). Any population of objects injected into the inner Solar System will naturally be pumped to the observed inclination distribution.

Wetherill (1988) also pointed out that high-eccentricity objects (specifically,  $a > 2.2$  AU and  $q < 0.8$  AU) seemed to be in short supply in his simulations; however, we believe this to be an artifact of the Öpik–Arnold Monte Carlo model, which did not allow for the variety of eccentricity pumping mechanisms to  $e > 0.5$  provided by resonant phenomena. Figure 11 shows an approximation to the steady-state distribution in perihelion/semimajor axis space, computed from a 1000-particle sample begun in the 3:1 mean-motion resonance (Gladman *et al.* 1997), to be compared with Wetherill (1988, Fig. 3) or Rabinowitz (1997, Fig. 5). The “real” dynamics populate the high eccentricity regions of orbital element space much more efficiently than the Monte-Carlo models predicted, and in particular supply a very strong signature from the resonance at 2.5 AU. While the latter feature is specific to a supply source from the 3:1 resonance, the elevated production of high  $e$  objects is generic to the process of escaping from the asteroid belt since the resonances are generically “passed” through at least once for all escaping asteroids. Also of note in Fig. 11 is the

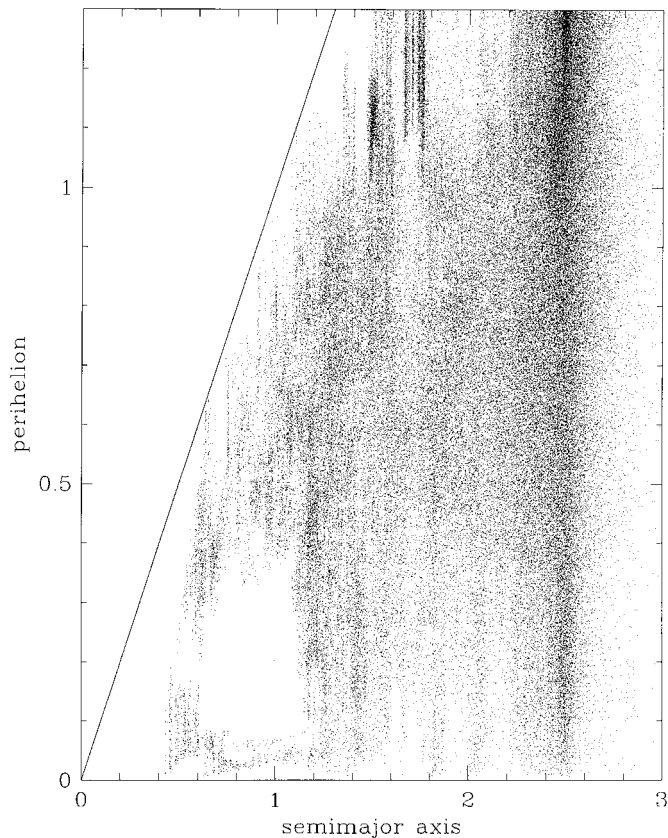


**FIG. 11.** Steady-state  $a/q$  distribution of NEOs coming from the 3:1 mean-motion resonance. The line shows the circular orbits; points to the upper left are unphysical. The obvious vertical band at 2.5 AU is the signature of the 3:1 resonance. Note the particles with  $a < 2$  AU that are decoupled from Earth via resonances ( $q > 1$ ) and the many objects with  $a > 2.2$  AU and high eccentricities ( $q < 0.8$  AU). The percentages of steady-state Anon, Aten, Apollo, and Amors ( $q < 1.3$  AU) in this figure are 1, 2, 71, and 26, respectively.

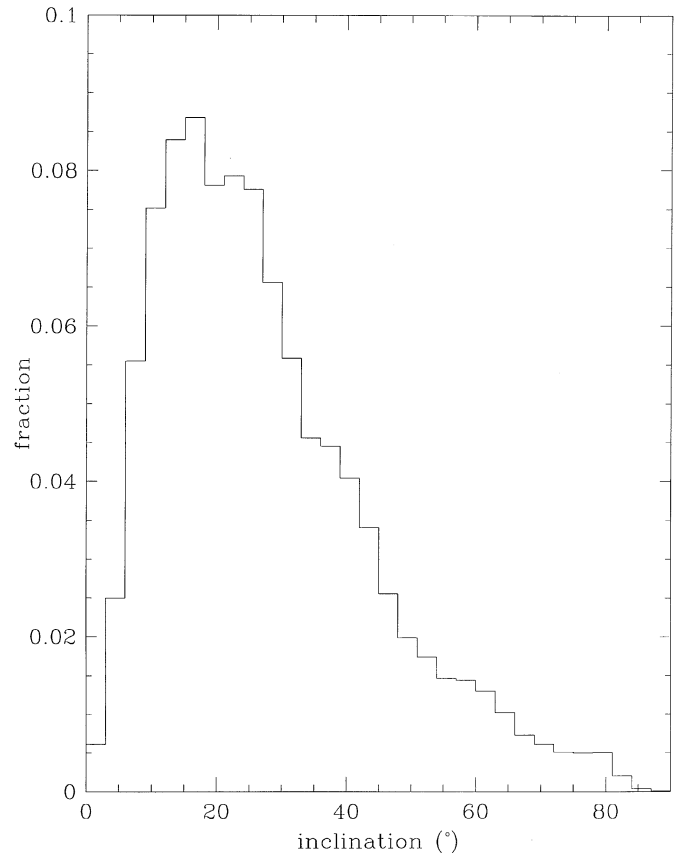


**FIG. 12.** Steady-state inclination distribution of NEOs coming from the 3:1 mean-motion resonance. The fraction of high inclination objects shown by this distribution is expected to be elevated with respect to the real NEOs due to detection biases against finding such objects.

existence of concentrations of objects in the Amor region between  $a = 1.3$  AU and  $a = 1.8$  AU, produced mostly by extractions from Earth-crossing space via the  $\nu_3$  and  $\nu_4$  resonances; this feature also appears to be present in the orbital distribution of Earth-approaching asteroids (Rabinowitz 1997, Fig. 7b). The steady-state inclination distribution produced by this 3:1 source is shown in Fig. 12, which is grossly similar to the observed distribution as shown in Weissman *et al.* (1989).

This brings us back to the question of cometary component of the NEO population. At this point we see no *dynamical* reason to require a cometary input component. Recent progress in understanding the expulsion of asteroids from the main belt illustrates that more abundant mechanisms exist for supplying the NEO population than previously discussed, through the channels of the main resonances (reviewed in Gladman *et al.* 1997), the Mars-crossing population (Migliorini *et al.* 1998), and the latter’s gradual replenishment from the main belt by the so-called “three-body” resonances (Nezvnorný and Morbidelli 1998, Murray *et al.* 1998). Thus, the previously calculated supply fluxes are probably lower limits, implying that almost all NEOs could come from an asteroidal source.

However, Encke exists. It is always troubling to argue from statistics of one, although Wetherill (1988), Weissmann *et al.* (1989), and Lupishko and Di Martino (1998) convincingly argue on spectroscopic grounds that there are other extinct cometary objects present in the population. Our opinion on the issue is that it is extremely unlikely that two utterly different sets of delivery physics (collisions and resonances for asteroids from a main-belt source versus Jupiter encounters and nongravitational forces for comets from a Kuiper Belt source) could fortuitously give NEO injection rates within a factor of three of each other, much less equality. Since it seems that asteroids can supply the input flux in quantitative and relatively complete models, while cometary input models have to be pushed to supply even half the NEOs, the former are likely to make up the bulk of the population.

We feel that the most likely way to make progress is to construct more complete models of the steady-state orbital distribution from various possible sources, and combine these with observational biases in an attempt to find the best match, taking into consideration estimates for the injection rate from these sources (although a complete fit of the steady-state orbit distribution could in principle *determine* the relative input rates). Further remote-sensing observations of near-Earth objects will of course also provide valuable information, although it is unclear how volatile-rich asteroids should differ from low-activity comets. Of course, the best answer is to go and land on many NEOs and see what fraction of them are cometary, but this is unlikely to happen anytime in the near future.

### ACKNOWLEDGMENTS

We thank H. Levison for providing us with the sample of initial conditions. We thank B. Bottke, A. Morbidelli, and G. Valsecchi for helpful discussions and L. Dones for comments as a reviewer.

### REFERENCES

- Boattini, A., and A. Carusi 1998. Atens: Importance among near-Earth asteroids and search strategies. *Vistas Astron.* **41**, 527–541.
- Bottke, W. F., and R. Greenberg 1993. Asteroidal collision probabilities. *J. Geophys. Res.* **20**, 878–881.
- Bottke, W. F., M. Nolan, R. Greenberg, and R. Kolvoord 1994. Collisional lifetimes and impact statistics of near-Earth asteroids. In *Hazards due to Comets and Asteroids* (T. Gehrels, Ed.), pp. 337–358. Univ. Arizona Press, Tucson.
- Bottke, W. F., M. C. Nolan, H. J. Melosh, A. M. Vickery, and R. Greenberg 1996. Origin of the Spacewatch small Earth-approaching asteroids. *Icarus* **122**, 406–427.
- Bottke, W. F., D. Richardson, and S. G. Love 1998. Production of Tunguska-sized bodies by Earth's tidal forces. *Planet. Space Sci.* **46**, 311–322.
- Bowell, E., K. Muinonen, and L. H. Wasserman 1994. A public-domain asteroid data base. In *Asteroids, Comets, Meteors* (A. Milani, M. DiMartino, and A. Cellino, Eds.), pp. 477–481. Kluwer, Dordrecht, Netherlands.
- Chapman, C., J. G. Williams, and W. K. Hartmann 1978. The asteroids. *Annu. Rev. Astron. Astrophys.* **16**, 33–75.
- Chyba, C. 1993. Explosions of small Spacewatch objects in the Earth's atmosphere. *Nature* **363**, 701–703.
- Dones, L., B. Gladman, H. J. Melosh, B. Tonks, H. Levison, and M. Duncan 1999. A comparison of Öpik-Arnold Monte Carlo methods with direct integrations. *Icarus* **142**, 509–524.
- Farinella, P., and D. R. Davis 1994. Collision rates and impact velocities in the main asteroid belt. *Icarus* **97**, 111–123.
- Farinella, P., Ch. Froeschlé, C. Froeschlé, R. Gonzi, G. Hahn, A. Morbidelli, and G. B. Valsecchi 1994. Asteroids falling into the Sun. *Nature* **371**, 314–317.
- Gladman, B. 1997. Destination Earth: Martian meteorite delivery. *Icarus* **130**, 228–246.
- Gladman, B. J., F. Migliorini, A. Morbidelli, V. Zappalà, P. Michel, A. Cellino, Ch. Froeschlé, H. Levison, M. Bailey, and M. Duncan 1997. Dynamical lifetimes of objects injected into asteroid belt resonances. *Science* **277**, 197–201.
- Greenberg, R., and M. Nolan 1989. Delivery of asteroids and meteorites to the inner Solar System. In *Asteroids II* (R. Binzel, T. Gehrels, and M. S. Matthews, Eds.), pp. 778–804. Univ. of Arizona Press, Tucson.
- Harris, N. W., and M. E. Bailey 1996. The cometary component of the near-Earth object population. *Irish Astron. J.* **23**, 151–156.
- Harris, N. W., and M. E. Bailey 1998. Dynamical evolution of cometary asteroids. *Mon. Not. R. Astron. Soc.* **297**, 1227–1236.
- Jedicke, R., and T. Metcalfe 1998. The orbital and absolute magnitude distributions of main belt asteroids. *Icarus* **131**, 245–260.
- Laskar, J. 1990. The chaotic motion of the Solar System. *Icarus* **88**, 266–291.
- Levison, H., and M. Duncan 1994. The long-term behavior of short-period comets. *Icarus* **108**, 18–36.
- Lupishko, D. F., and M. Di Martino 1998. Physical properties of near-Earth asteroids. *Planet. Space Sci.* **46**, 47–74.
- Marsden, B., Z. Sekanina, and D. Yeomans 1973. Comets and nongravitational forces. *V. Astrophys. J.* **78**, 211–225.
- Menichella, M., P. Paolicchi, and P. Farinella 1996. The main belt as a source of near-Earth asteroids. *Earth Moon Planets* **72**, 133–149.
- Michel, P. 1997. Effects of linear secular resonances in the region of semimajor axes smaller than 2 AU. *Icarus* **129**, 348–366.
- Michel, P., and Ch. Froeschlé 1997. The location of secular resonances for semimajor axes smaller than 2 AU. *Icarus* **128**, 230–240.
- Michel, P., and F. Thomas 1996. The Kozai resonance for near-Earth Asteroids with semimajor axes smaller than 2 AU. *Astron. Astrophys.* **307**, 310–318.
- Michel, P., F. Migliorini, A. Morbidelli, and V. Zappalà 2000. The population of Mars-crossers: Classification and dynamical evolution. *Icarus* **145**, 332–347.
- Michel, P., V. Zappalà, A. Cellino, and P. Tanga 2000. Estimated abundance of Atens and asteroids evolving on orbits between Earth and Sun. *Icarus* **143**, 421–424.
- Migliorini, F., P. Michel, A. Morbidelli, D. Nesvorný, and V. Zappalà 1998. Origin of multikilometer Earth- and Mars-crossing asteroids: A quantitative simulation. *Science* **281**, 2022–2024.
- Milani, A., M. Carpino, G. Hahn, and A. Nobili 1989. Dynamics of planet-crossing asteroids: Classes of orbital behavior. *Icarus* **78**, 212–269.
- Milani, A., M. Carpino, and F. Marzari 1990. Statistics of close approaches between asteroids and planets: Project SPACEGUARD. *Icarus* **88**, 292–335.
- Morbidelli, A., and B. Gladman 1998. Orbital and temporal distribution of meteorites originating in the asteroid belt. *Met. Plan. Sci.* **33**, 999–1016.
- Morbidelli, A., and J. Henrard 1991. Secular resonances in the asteroid belt: Theoretical perturbation approach and the problem of their location. *Celest. Mech.* **51**, 131–167.
- Morrison, D., C. Chapman, and P. Slovic 1994. The impact hazard. In *Hazards Due to Comets and Asteroids* (T. Gehrels, Ed.), pp. 59–91. Univ. of Arizona Press, Tucson.
- Murray, N., M. Holman, and M. Potter 1998. On the origin of chaos in the asteroid belt. *Astron. J.* **116**, 2583–2589.
- McKinnon, W. B., K. Zahnle, B. Ivanov, and H. J. Melosh 1997. Cratering on Venus: Models and observations. In *Venus II* (S. W. Bougher, D. M. Hunten, and R. J. Phillips, Eds.), pp. 969–1014. Univ. Arizona Press, Tucson.

- Nesvorný, D., and A. Morbidelli 1998. Three-body mean motion resonances and the chaotic structure of the asteroid belt. *Astron. J.* **116**, 3029–3037.
- Öpik, E. J. 1963. Survival of comet nuclei and the asteroids. *Adv. Astron. Astrophys.* **2**, 219–262.
- Öpik, E. J. 1976. *Interplanetary Encounters*. Elsevier, New York.
- Rabinowitz, D. 1997. Are main-belt asteroids a sufficient source for the Earth-approaching asteroids? I. Predicted vs observed orbital distributions. *Icarus* **127**, 33–54.
- Rabinowitz, D., E. Helin, K. Lawrence, and P. Steven 2000. A reduced estimate of the number of kilometre-sized near-Earth asteroids. *Nature* **403**, 165–166.
- Rabinowitz, D., E. Bowell, E. Shoemaker, and K. Muinonen 1994. The population of Earth-crossing asteroids. In *Hazards du to Comets and Asteroids* (T. Gehrels, Ed.), pp. 285–312. Univ. Arizona Press, Tucson.
- Rabinowitz, D., T. Gehrels, J. V. Scotti, R. McMillan, M. Perry, W. Wisniewski, S. Larson, E. Howell, and B. Mueller 1993. Evidence for a near-Earth asteroid belt. *Nature* **363**, 704–706.
- Shoemaker, E. M., J. G. Williams, E. F. Helin, and R. E. Wolfe 1979. Earth-crossing asteroids: Orbital classes, collision rates with Earth, and origin. In *Asteroids* (T. Gehrels, Ed.), pp. 253–282. Univ. of Arizona Press, Tucson.
- Steel, D. I., and D. J. Asher 1996. On the origin of comet Encke. *Mon. Not. R. Astron. Soc.* **281**, 937–944.
- Steel, D. I., and W. J. Baggeley 1985. Collisions in the Solar System. I. Impacts of the Apollo–Amor–Aten asteroids upon the terrestrial planets. *Mon. Not. R. Astron. Soc.* **212**, 817–836.
- Tholen, D., and R. J. Whiteley 1998. Results from NEO searches at small solar elongation. *Bull. Am. Astron. Soc.* **30**, 1041. [Abstract]
- Valsecchi, G., A. Morbidelli, R. Gonczi, P. Farinella, Ch. Froeschlé, and Cl. Froeschlé 1995. The dynamics of objects in orbits resembling that of P/Encke. *Icarus* **118**, 169–180.
- Valsecchi, G. 1999. From Jupiter-family comets to objects in Encke-like orbits. In *Evolution and Source Regions of Asteroids and Comets* (J. Svoren, E. M. Pritich, and H. Rickman, Eds.), pp. 353–364. IAU Colloquium 173. Astron. Inst. of the Slovak Academy of Sciences, Tatranská Lomnica, Slovak Republic.
- Weissman, P., M. A'Hearn, L. McFadden, and H. Rickman 1989. Evolution of comets into asteroids. In *Asteroids II* (R. Binzel, T. Gehrels, M. S. Matthews, Eds.), pp. 880–920. Univ. of Arizona Press, Tucson.
- Wetherill, G. 1979. Steady state populations of Apollo–Amor objects. *Icarus* **37**, 96–112.
- Wetherill, G. 1988. Where do the Apollo objects come from? *Icarus* **76**, 1–18.
- Wetherill, G. 1989. Cratering of the terrestrial planets by Apollo objects. *Meteoritics* **24**, 15–22.
- Wetherill, G. W. 1967. Collisions in the asteroid belt. *J. Geophys. Res.* **72**, 2429–2444.
- Whiteley, R. J., and D. Tholen 1998. A CCD search for Lagrangian asteroids of the Earth–Sun system. *Icarus* **136**, 154–167.
- Wisdom, J., and M. Holman 1991. Symplectic maps for the N-body problem. *Astron. J.* **102**, 1528–1538.